Journal of Applied Polymer Science

A Surface Analysis of Polypropylene/Clay Nanocomposites Exposed to Electron Irradiation

Ahmad Asadinezhad,[1] Hossein Ali Khonakdar,[2] Seyed Hassan Jafari,[3] Frank Simon,[4] Udo Wagenknecht[4]

[1]Department of Chemical Engineering, Isfahan University of Technology, 84156-83111, Isfahan, Iran
[2]Department of Polymer Processing, Iran Polymer and Petrochemical Institute, 14965-115, Tehran, Iran
[3]School of Chemical Engineering, College of Engineering, University of Tehran, 11155-4563, Tehran, Iran
[4]Leibniz-Institut für Polymerforschung Dresden e.V., D-01069, Dresden, Germany
Correspondence to: H. A. Khonakdar (E-mail: hakhonakdar@gmail.com)

ABSTRACT: The effects of electron irradiation in air at various doses on surface chemical composition of nanofilled polypropylene were explored by X-ray photoelectron spectroscopy. An organically modified nanoclay ingredient along with a functional compatibilizer was employed for this purpose. The nanocomposite formation was confirmed by means of transmission electron microscopy, where in presence of compatibilizer, an exfoliated structure was brought about. Medium irradiation dose was established to be considerably effective in raising surface oxygen content, while at very high electron beam fluence, the ablation (etching) predominated. The optimal electron beam intensity was also found with respect to the extent of the functionalization. Various moieties of ether, ester, and alcohol characteristics were produced after exposure which could act as functional, active precursors being suitable for subsequent functionalization reactions. Furthermore, it could be understood that the electron irradiation spur organoclay migration toward surface layers. © 2012 Wiley Periodicals, Inc. J. Appl. Polym. Sci. 000: 000–000, 2012

KEYWORDS: surfaces and interfaces; irradiation; nanostructured polymers

Received 7 June 2012; accepted 6 July 2012; published online
DOI: 10.1002/app.38314

INTRODUCTION

The properties of the polymer surfaces are largely controlled by chemistry of the surface layer. A number of techniques have been devised to tune and analyze materials surfaces and found many benefits in different applications.[1] The surface modification of polymers by means of ionizing radiation has been known for decades and yet is a subject of intensive research.[2] Irradiation brings on a series of chemical reactions involving functionalization, crosslinking, and etching which all occur at the surface to the extent depending on the irradiation dose and the working gas. As the penetration depth of the ionizing beam is on the order of micrometers, only the near-surface region (top nanolayer) is modified and the bulk remains unchanged.[3] The outcome of the surface modifications can then be exploited in many applications such as biomedical ones.

Recently, several homopolymers have been improved in performance thanks to the incorporation of the active, nanofillers.[4] This also holds for polypropylene (PP), where due to the inherent incompatibility with some nanoparticles, an interfacial modifier is occasionally employed to increase phase adhesion. PP/Clay nanocomposites which are esteemed nowadays as novel materials of successful performance,[5] suffer from undesired surface properties such as low affinity toward synthetic/natural entities. This can be dealt with somewhat via irradiation techniques. Few reports have yet been devoted to surface modification of the nanofilled polymers.[6–9] Poly(carbonate-urea) urethane copolymer films were treated via plasma in oxygen and increased adhesion, coverage, and growth of human umbilical vein endothelial cells were demonstrated.[6] Also, UV irradiation of the same material revealed that the adhesion and proliferation of the human umbilical vein endothelial cell line was considerably promoted upon irradiating with UV rays under nitrogen and oxygen ambient.[7] The UV exposure changed the surface from amphiphilic to hydrophilic while preserving the morphology. Elsewhere,[8] argon ion bombardment on the surface of carbon-titanium nanocomposite films was performed and observed that after the ion bombardment, the oxygen atoms were selectively bonded to titanium atoms. Also, a preferential sputtering of the amorphous phase was detected leading to the emergence of carbon/titanium nanocrystallites on film surface. The oxygen plasma treatment of nanocomposite hybrid polymer thin films

based on poly(methyl methacrylate) copolymers was found to be capable of converting the hydrophobic surface into hydrophilic within a short time.[9] Moreover, the exposure time needed for this conversion decreased as the oxygen content increased.

The primary focus of the current article is to understand the changes in surface chemistry of PP which arise subsequent to the electron beam exposure in the presence of nanoclay particles and compatibilizer. This was fulfilled by means of X-ray photoelectron spectroscopy (XPS) as a highly surface-sensitive, reliable technique and an ideal, most widely employed tool for the surface elemental quantification and chemical information.[10,11]

EXPERIMENTAL

Materials

The materials were all of commercial grade which were used as received. Isotactic PP, grade Moplen HP501H, was provided from Basell (Germany). Maleic anhydride grafted PP (PP-*g*-MA) was used as the compatibilizer from Chemtura. Cloisite15A, a natural montmorillonite modified with dimethyl bis(hydrogenated tallow) ammonium chloride, was employed as the nanoclay which was supplied by Southern Clay Products.

Sample Preparation and Treatment

PP/Clay/Compatibilizer samples in three formulations, 100/0/0 (neat PP), 95/5/0, and 90/5/5 (all in wt %) were prepared using melt blending technique. A corotating, twin screw extruder ZSK 30 (Werner & Pfeidlerer) was employed to prepare the samples at screw speed of 150 rpm. The extrusion temperature profile was set within 170°C–200°C from hopper to die. A hot laboratory press (Weber) was used to form melt-blended samples in thin sheet form. The samples were irradiated with low-energy electrons using the laboratory device ADU advanced electron beams (AEB). The samples were placed on a sample holder which was mounted on the conveyor system of the ADU and passed under the electron beam exit window with well adjusted velocity (50 ft/min) in order to apply the desired dose to the samples. The samples were irradiated with doses of 50, 100, 200, and 400 kGy at room temperature in air. The total absorbed dose was applied in steps of 6.25 kGy in order not to exceed the maximum temperature of the samples beyond 60°C. The energy of the electrons and beam current were 80 keV and 1 mA, respectively.

Characterizations

The extruded samples were ultramicrotomed down to 80 nm thickness under cryogenic conditions at −120°C via EM UC/FC6 ultramicrotome (Leica) equipped with a diamond knife. Transmission electron microscopy (TEM) images were taken using LEO 910 TEM (Carl Zeiss) at an accelerating voltage of 120 kV. XPS was performed on on an AXIS ULTRA photoelectron spectrometer (KRATOS ANALYTICAL). The spectrometer was equipped with a monochromatic Al Kα X-ray source of 300 W at 15 kV. The kinetic energy of the photoelectrons was determined with a hemispheric analyzer set to pass energy of 160 eV for wide scan spectra and 20 eV for high-resolution spectra. During all measurements, the electrostatic charging of the sample was over-compensated by means of a low-energy electron source working in combination with a magnetic immersion lens. Later, all recorded peaks were shifted by the same amount which was necessary to set the C1s peak to 285.0 eV for saturated hydrocarbons. Quantitative elemental compositions were determined from peak areas using experimentally determined sensitivity factors and the spectrometer transmission function. Spectrum background was subtracted according to the Shirley method.[12] The high-resolution spectra were deconvoluted by means of a computer routine. Free parameters of component peaks were their binding energy, height, full width at half maximum and the Gaussian-Lorentzian ratio.

RESULTS AND DISCUSSION

Bulk Morphology

TEM images of two additive-containing PP samples in various magnifications are shown in Figure 1. The nanoclay moieties are dispersed at nanoscale in PP matrix which ensures the nanocomposite formation. As for PP/clay/compatibilizer 95/5/0 sample, the nanoclay is observed in form of tactoids (spindle-like platelets stacks) which point to the high interfacial tension between PP and nanosize organoclay phases.[13] Upon addition of the compatibilizer by 5 wt % (PP/clay/compatibilizer 95/5/5), a major part of the clay tactoids disappear and the interlayer distance as well as the extent of the exfoliation increase. These indicate a better and much finer dispersion. This is clearly visible from TEM micrographs and suggests the enhanced affinity between PP and organoclay components as a consequence of the functional compatibilizer incorporation. Similar finding has also been reported on blend nanocomposites.[14]

Surface Chemistry

The elemental ratios of three key elements (C1s, O1s, and N1s) of the samples calculated from normalized areas of the element peaks are shown in Table I. Regarding the neat PP sample, carbon constitutes the major element of the surface layer of the untreated sample (0 kGy), even though traces of oxygen is also detected on the sample surface which can be due to the moieties of auto-oxidized PP or nonspecifically adsorbed impurities. Upon electron exposure at 50 kGy, the oxygen concentration is increased and trace amount of nitrogen is indentified as well. Surface enrichment in oxygen continues as the irradiation dose is raised up to 100 KGy. The trend sustains up to 200 kGy beam fluence, where the highest oxygen quantity is reached. Such a multiple increase in oxygen concentration which is parallel to a decrease in carbon content is ascribed to the surface functionalization.[15,16] However, at a very high dose (400 kGy), due to intensive irradiation, the ablation occurs and a decrease in oxygen and nitrogen content is observed. Alteration in surface composition is well depicted in Figure 2, where [O] : [C] ratio as a function of the electron beam fluence is plotted. The intensity of 200 kGy is realized as the optimal dose where the surface modification reaches a desirable level.

The electron beam of medium intensity is composed of energetic particles which can generate metastable species upon colliding with the surface layer particles. In presence of the ambient oxygen, the oxygen-congaing moieties can then be formed. At very high electron beam intensity, the formation of carbon–carbon crosslinked structures as well as etching of the surface particles is more favorable than the formation of the new functionalities.[17,18] The identity of the oxygen-containing functionalities can be

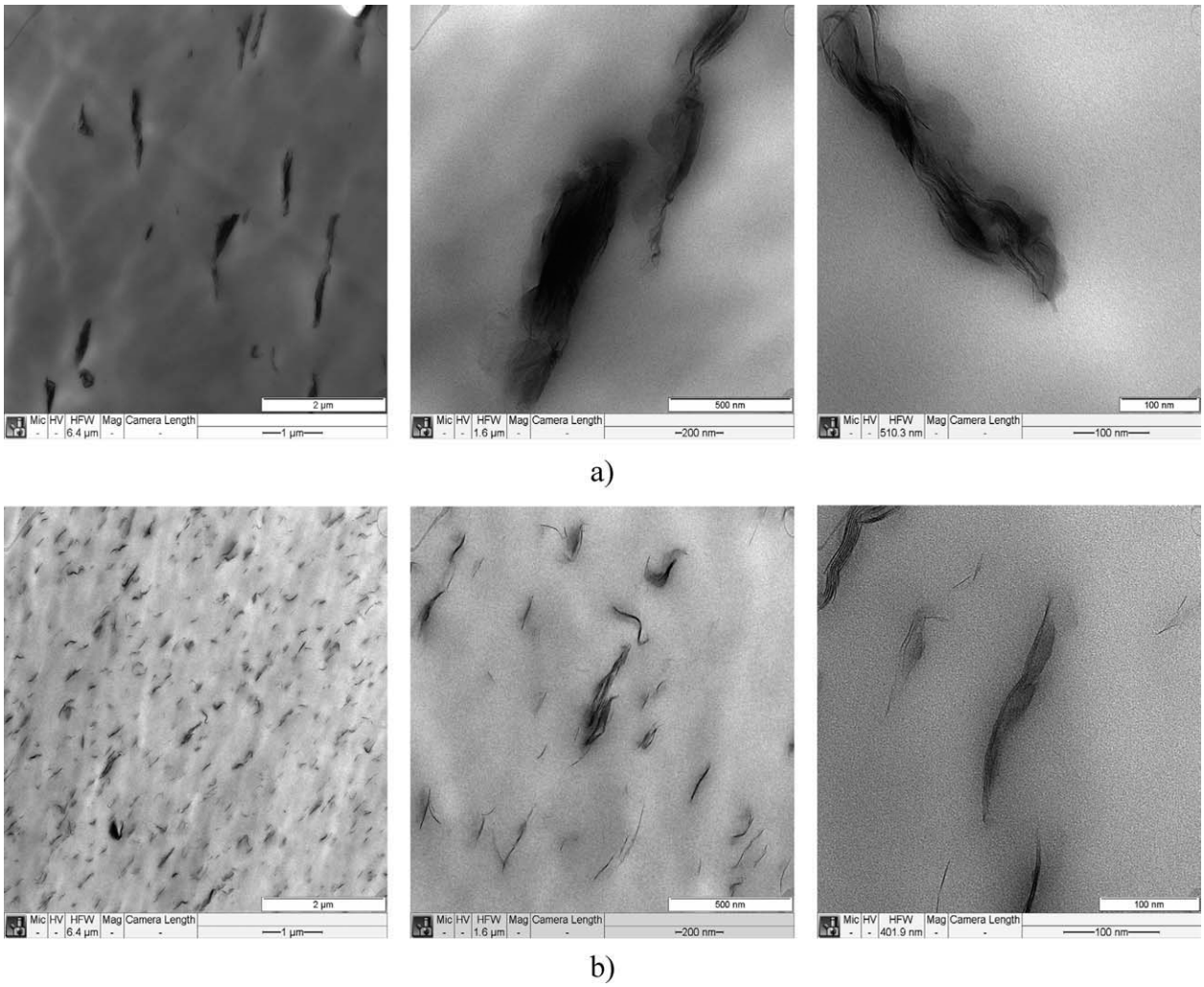

Figure 1. TEM micrographs of PP/Cloisite 15A 95/5 at different magnifications, a) without compatibilizer; b) with 5 wt % compatibilizer (Elvaloy PTW).

examined via C1s high-resolution spectra which are displayed in Figure 3. The untreated sample reveals C1s peak at the binding energy of 285 eV. After electron irradiation exposure, minor shoulders to the main peak characteristic to C—O bond arise. The deconvolution of C1s peak indicates two additional component peaks of weak magnitude at around 286 and 288 eV. If it is

Table I. Surface Elemental Concentration of the Neat PP Sample Irradiated via Electron Beam at Different Fluence

Irradiation intensity (KGy)	[C] atomic conc. (%)	[O] atomic conc. (%)	[N] atomic conc. (%)	[O] : [C]	[N] : [C]
0 (untreated)	98.98	0.25	–	0.0025	–
50	91.71	1.07	0.22	0.0178	0.0024
100	89.94	2.87	–	0.0319	–
200	70.62	4.66	0.29	0.0660	0.0041
400	86.73	2.82	–	0.0325	–

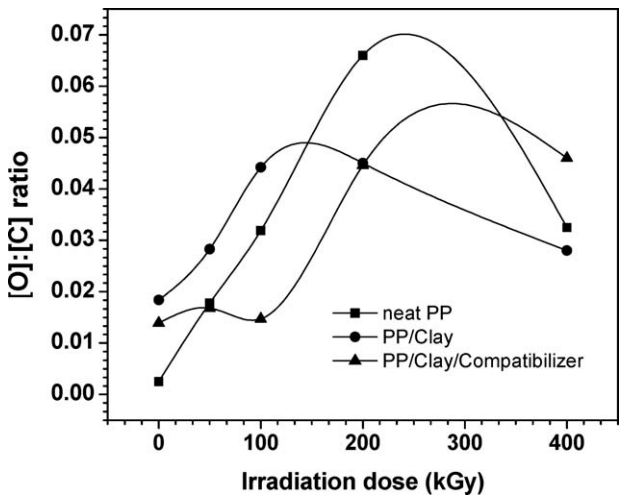

Figure 2. The ratio of [O] : [C] for different samples as a function of electron irradiation intensity indicating surface composition.

Applied Polymer SCIENCE

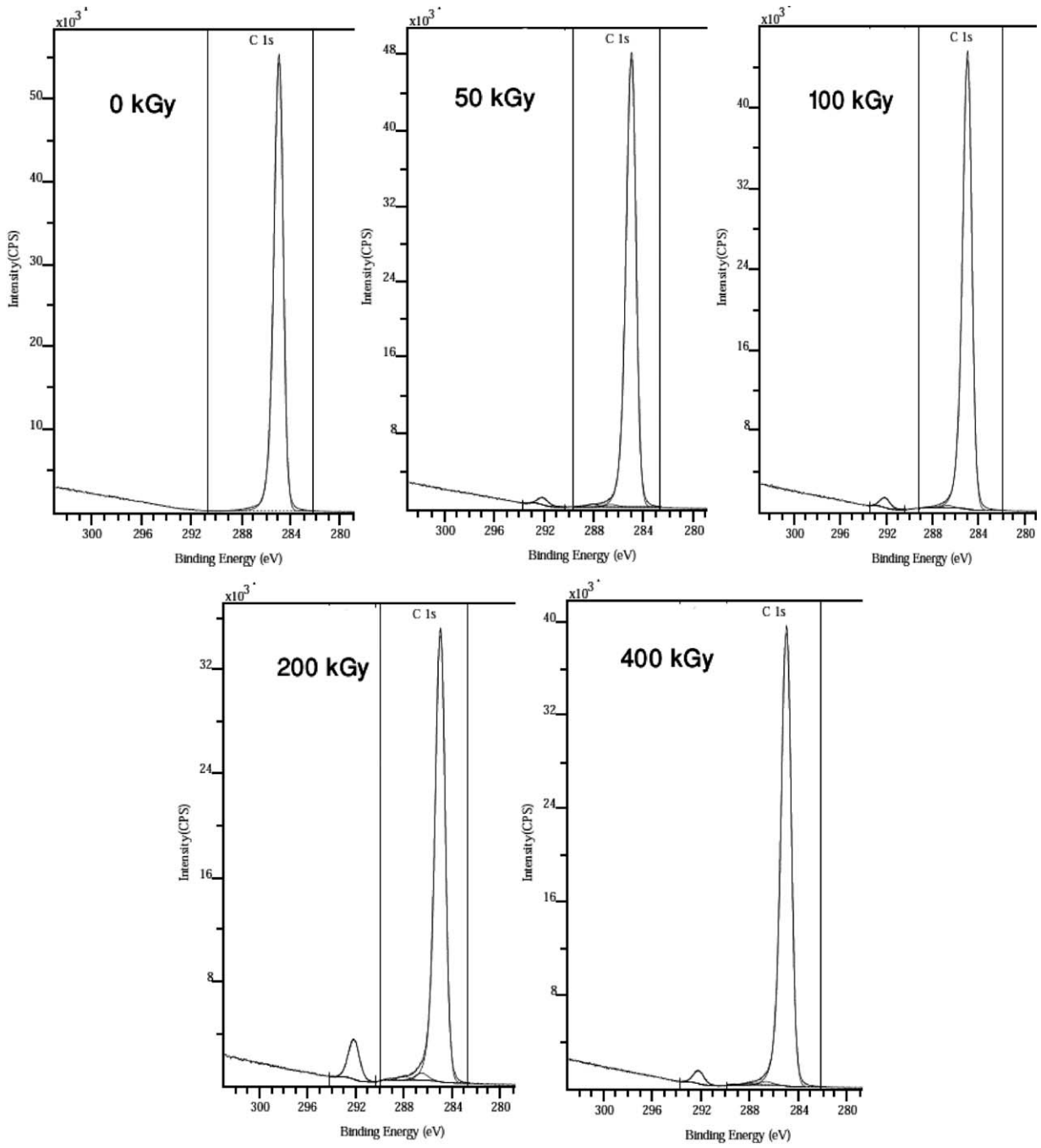

Figure 3. High resolution C1s signals of neat PP sample recorded at different electron doses along with deconvoluted peaks indicating surface chemical state.

considered that the component peak at about 288 eV represents the carbonyl atoms of the ester functionality (O=C—O—C), the component at about 286 eV then shows the alcohol-sided carbon atoms of the ester groups (O=C—O—C).[19,20] According to the stoichiometry of the ester functionality, the two component peaks must have the same intensity. The excess component peaks at about 286 eV indicate the presence of alcohol (C—OH) and/or ether groups (O—C—O).[20,21] It is worth noting that the magnitude of the component peaks, which correspond to the number of functional groups introduced in the sample surfaces, depends on the electron irradiation dose.

As for the second sample series where the organoclay Cloisite 15A is incorporated, the XPS analysis detects moieties of nitrogen and oxygen which in principle are originated from the quaternary ammonium and hydrogenated tallow groups of the nanoclay. The respective data are shown in Table II. Upon irradiating the sample with electron beam, the concentration of oxygen and nitrogen increases. Such an increase in oxygen content can be attributed to the formation of oxygen-containing functional groups. In connection with the observed increase in nitrogen, it is likely that nanoclay migrates from the polymer matrix to the surface as a result of electron irradiation. As a

matter of fact, the high energy input from the electron beam is able to compensate the counteracting driving force, which minimizes the surface free energy by enriching the polymer surface from the least available polar sequences. However, further and more specific analysis should be done to verify this phenomenon.

Further increase in oxygen content is achieved on increasing irradiation flux, where the highest oxygen concentration is obtained at the dose of 200 kGy. This is graphically shown in Figure 2, where the maximum fraction of [O] : [C] is attained at 200 kGy. The nitrogen content also increases in quantity as the driving force for the nanoclay migration is strengthened. On the other hand, at more intensive irradiation (400 kGy), due to ablation and etching, lower amounts of the nitrogen and oxygen elements are found at the surface. The deconvolution of the corresponding high-resolution C1 s spectra shows the presence of alcohol, ether, and ester groups on the sample surfaces by the similar reasoning given on the previous sample.

Table III shows the quantitative XPS analysis of the nanoclay-containing PP samples, where an interfacial modifier (compatibilizer) is also included in the formulation. Oxygen and nitrogen are found on the surface due to the presence of the compatibilizer and the organoclay nanoparticles. An increase in oxygen content is identified after irradiating the sample with an electron dose of 50 kGy. Although, no considerable difference in elemental concentration is evidenced upon increasing the irradiation dose to 100 kGy, much enhancement is observed after exposing the sample to the intensity of 200 kGy. This is well communicated through [O] : [C] ratios by three order of magnitude increase (see Figure 2). It is also seen that the irradiation has stronger impact on the [O] : [C] ratio of the neat sample compared to the other two which imply that the clay and compatibilizer exert some restriction on the level of the effects of the electron beam. In addition, nitrogen is also detected in higher content which may be associated with the nanoclay diffusion to the surface layers as discussed before. At more elevated electron beam flux (400 KGy); no sensible change is found in oxygen content where the ablation counterbalances the functionalization.

It is critical to note that the presence of oxygen-containing additives may challenge the findings as to whether the enhancement in oxygen content is chiefly induced from functionalization or migration of the oxygen-containing ingredients. The issue of how far the electron irradiation can affect the migration of the additives would be addressed in our forthcoming effort.

Table II. Surface Elemental Concentration of PP/Nanoclay 95/5 Irradiated via Electron Beam at Different Fluence

Irradiation intensity (KGy)	[C] atomic conc. (%)	[O] atomic conc. (%)	[N] atomic conc. (%)	[O]:[C]	[N]:[C]
0 (untreated)	89.99	1.66	0.15	0.0184	0.0017
50	91.52	2.59	0.25	0.0283	0.0027
100	91.80	4.06	-	0.0442	-
200	94.10	4.23	0.16	0.0450	0.0017
400	89.79	2.52	-	0.0280	-

Table III. Surface Elemental Concentration of PP/Nanoclay/Compatibilizer 95/5/5 Irradiated via Electron Beam at Different Fluence

Irradiation intensity (KGy)	[C] atomic conc. (%)	[O] atomic conc. (%)	[N] atomic conc. (%)	[O] : [C]	[N] : [C]
0 (untreated)	96.08	1.34	0.26	0.0139	0.0027
50	95.73	1.61	-	0.0168	-
100	95.94	1.41	-	0.0147	-
200	93.49	4.17	0.85	0.0446	0.0090
400	87.81	4.04	-	0.0460	-

CONCLUSIONS

This work concerns preparation and surface characterization of the nanoclay-filled polypropylene in presence of the compatibilizer. TEM reveals that the compatibilizer could stabilize the morphology by delivering an exfoliated structure compared to the sample without the compatibilizer. Also, the electron irradiation is efficiently able to alter the surface chemistry desirably. This is a consequence of functionalization-ablation competing reactions where at medium electron beam fluence, oxygen-containing active groups are generated on the surface while at very high dose; the etching of the surface layers dominates. Moreover, it seems that the electron irradiation can contribute to the driving force of the organoclay migration toward surface layers.

ACKNOWLEDGMENTS

H.A. Khonakdar greatly appreciates the financial support from Alexander von Humboldt foundation.

REFERENCES

1. Morent, R.; De Geyter, N.; Desmet, T.; Dubruel, P.; Leys, C. *Plasma. Process. Polym.* **2011,** *8*, 171.
2. Hasebe, T.; Nagashima, S.; Yoshimoto, Y.; Hotta, A.; Suzuki, T. *Nucl. Instrum. Meth. B.* **2012,** *282*, 134.
3. García, J. L.; Asadinezhad, A.; Pacherník, J.; Lehocký, M.; Junkar, I.; Humpolíček, P.; Sáha, P.; Valášek, P. *Molecules* **2010,** *15*, 2845.
4. Khonakdar, H. A.; Jafari, S. H.; Asadinezhad, A. *Iran. Polym. J.* **2008,** *17*, 19.
5. Manias, E.; Touny, A.; Manias, E.; Touny, A. *Chem. Mater.* **2001,** *13*, 3516.
6. Solouk, A.; Cousins, B. G.; Mirzadeh, H.; Seifalian, A. M. *Biotechnol. Appl. Bioc.* **2011,** *58*, 147.
7. Olbrich, M.; Punshon, G.; Frischauf, I.; Salacinski, H. J.; Rebollar, E.; Romanin, C.; Seifalian, A. M.; Heitz, J. *J. Biomater. Sci. Polym. Ed.* **2007,** *18*, 453.
8. El Mel, A. A.; Angleraud, B.; Gautron, E.; Granier, A.; Tessier, P. Y. *Thin Solid Films* **2011,** *519*, 3982.

9. Augustine, B. H.; Hughes, W. C.; Zimmermann, K. J.; Figueiredo, A. J.; Guo, X.; Chusuei, C. C. *Langmuir* **2007,** *23*, 4346.
10. Ulvskov, P. Plant Polysaccharides: Biosynthesis and Bioengineering; Wiley: New York, **2010.**
11. Dwivedi, N.; Kumar, S.; Malik, H. K.; Kumar, C. S.; Dayal, S.; Rauthan, C. M. S.; Panwar, O. S. *J. Phys. Chem. Sol.* **2012,** *73*, 308.
12. Repoux, M. *Surf. Interface Anal.* **1992,** *18*, 567.
13. Rosoff, M. Nano-Surface Chemistry; Marcel Dekker: New York, **2001.**
14. Boudenne, A.; Ibos, L.; Candau, Y. Handbook of Multiphase Polymer Systems; Wiley Interscience: New York, **2011.**
15. Vrlinič, T.; Vesel, A.; Cvelbar, U.; Kranjc, M.; Mozetic, M. *Surf. Interface Anal.* **2007,** *39*, 476.
16. Calvimontes, A.; Mauersberger, P.; Nitschke, M.; Dutschk, V.; Simon, F. *Cellulose* **2011,** *18*, 803.
17. Bhowmick, A. K.; Majumder, P. J.; Banik, I. *Macromol. Symp.* **1999,** *143*, 21.
18. Pawdeh, S. M.; Parab, S. *J. Appl. Polym. Sci.* **2011,** *119*, 1220.
19. Kodolov, V. I.; Shabanova, I. N.; Babushkina, S. N.; Chirkova, E. I.; Keller, N. V. *J. Struct. Chem.* **1998,** *39*, 912.
20. Seong, H. J.; Boehmann, A. L. *Energ. Fuel.* **2011,** *25*, 602.
21. Beamson, G.; Briggs, D. *Surf. Interface Anal.* **1992,** *39*, 476.